ANNALS OF GEOPHYSICS, 68, 1, V111, 2025; doi:10.4401/ag-9173
OPEN ACCESS

A target-based, multi-hazard assessment approach as a tool for supporting decision-making in volcanic areas: a case study in Mt. Etna, Italy

Alexander Garcia[*,1], Laura Sandri[1], Vera Pessina[2], Fabrizio Meroni[2], Elisa Varini[3], Annalisa Cappello[4]

(1) Istituto Nazionale di Geofisica e Vulcanologia, Sezione di Bologna, Bologna, Italy
(2) Istituto Nazionale di Geofisica e Vulcanologia, Sezione di Milano, Milano, Italy
(3) Consiglio Nazionale delle Ricerche, Istituto di Matematica Applicata e Tecnologie Informatiche, Milano, Italy
(4) Istituto Nazionale di Geofisica e Vulcanologia, Osservatorio Etneo, Catania, Italy

Article history: received September 30, 2024; accepted January 17, 2025

Abstract

Multi-hazard assessment aims at evaluating the potential impacts of various natural and human-induced hazards in a given area of interest and time period. The analysis can include hazards of different nature – such as volcanic eruptions, earthquakes, floods, landslides, and industrial accidents – considering their interdependencies and cumulative effects. Multi-hazard assessments can provide critical insights into the potential impact of multiple hazards, enabling decision makers to adopt a wider view of the problem with respect to the approach of analyzing single hazards independently. Volcanoes are interesting targets for implementing multi-hazard analyses because they are intrinsically a multi-hazard source due to the variety of phenomena usually related to volcanic eruptions (e.g. volcano seismicity, lava flows, tephra fall, lahars, etc.). This paper presents a target-based approach for multi-hazard analysis at Etna volcano (Italy) in which the output of probabilistic single hazard assessment can be harmoniously integrated and used for assessing a wide number of scenarios. The findings underscore the advantages of adopting such a kind of approach for supporting decision makers when using the results of multiple probabilistic hazards assessments for performing tasks of planning, mitigation, or emergency preparedness. This work has been performed in the framework of the INGV project "Pianeta Dinamico" – PANACEA, a project developed for implementing multi-hazard and multi-risk assessments at Etna volcano.

Keywords: Multi-hazard; Lava flows; Tephra fallout; Seismicity; Fault tree; Poisson process; Milo

1. Introduction

Multi-hazard assessment (MHA) refers to the comprehensive evaluation of different hazards that can occur simultaneously or sequentially in a given region. This concept recognizes the interconnected nature of different hazards and aims to provide a general understanding to support the assessment of their potential impacts. Unlike single-hazard assessment,

which focus on one specific type of hazard, multi-hazard assessment needs to take into account the harmonization of different single hazards (such as earthquakes, tsunamis, landslides, floods, volcanic eruptions, and extreme weather events, among others), as well as to consider the complex interactions and cascading effects among them.

MHA aims at providing a theoretical framework for harmonizing the methodologies employed and the results obtained from hazard assessments by considering different independent hazards as well as the interactions and cumulative effects of multiple hazards (Marzocchi et al., 2012; Gasparini and Garcia-Aristizabal, 2014; Liu et al., 2015). Volcanoes are interesting targets for implementing multi-hazard analyses because they are intrinsically a multi-hazard source; indeed, volcanic eruptions are often characterized by different volcanic phenomena, as e.g. lava flows, tephra fallout, pyroclastic flows, volcanic earthquakes, etc., either occurring during different eruptive events or during the same eruption within relatively short time intervals, and each of these phenomena may threaten the surrounding areas in a different way. Moreover, beyond the specific volcanic activity, external hazard sources (e.g. extreme meteorological events – as rain, heat waves, droughts, etc. –, tectonic seismicity, landslides, etc.) can also threaten the same areas and can be taken into account as further independent hazards or in cascading effects, as they can interact among them and/or with volcanic hazards. Finally, MHA set the grounds for multi-risk assessment (MRA) which is becoming key factor for the development of a sustainable environment, sound land-use planning, and for implementing risk mitigation strategies. Indeed, in a MRA, the MHA can be integrated with (multi-dimensional) vulnerability allowing the assessment of risk interactions at both the hazard and vulnerability levels (see e.g. Marzocchi et al., 2012; Selva 2013; Gasparini and Garcia-Aristizabal, 2014; Liu et al., 2015). As a result, the risk due to a variety of phenomena can be harmonized and assessed using the same metrics, becoming in this way comparable and therefore an interesting tool for decision making. Considering in particular the volcanic areas, so far a number of MRA have been presented in the literature, demonstrating the potential of such kind of analyses (see e.g. Thierry et al., 2008; Marzocchi et al., 2012; Martín-Raya et al., 2024; Pessina et al., 2025).

MHA is indispensable for proper understanding and managing the complex risk landscape posed by natural hazards; however, different challenges must be faced to appropriately implement a full analysis: first, combining diverse datasets from different hazards poses a significant challenge due to differences in data quality, scale, and format. Second, effective MHA requires collaboration among experts in different disciplines, with different degrees of awareness about the approaches for hazard assessment, and such interaction could be not straightforward; third, each hazard is characterized by its own intensity measures, pertinent spatial scales, size distribution, and event rates. Therefore, developing a general methodology for MHA that can be straightforwardly used to support decision making is not an easy task.

In the literature, different attempts have been presented to aggregate multiple volcanic hazard assessments with the aim of supporting decision makers. In general terms, we can group most of these attempts in two wide groups, namely (i) aggregated volcanic hazard maps, which is probably the most common approach, and (ii) index-based approaches. Aggregated volcanic multi-hazard maps are generally based on (probabilistic) hazard assessment associated with scenarios of different hazardous volcanic phenomena, and the results of such analyses are overlaid, explicitly showing the common areas that can be affected by different hazards (usually for specific scenarios, such as, for example, events with a determined return period, or a 'characteristic' reference size). Recent examples of such analyses can be found, for example, in Weir et al. (2022) applied to the Taranaki Mounga volcano, New Zealand, where the authors defined a set of scenarios and, using deterministic modeling, defined the footprints of the different hazards, combining them in aggregated hazards outputs. Another recent example has been presented by Alcozer-Vargas et al. (2022) who performed a GIS-based multi-hazard assessment at the San Pedro volcano, northern Chile, for different volcanic phenomena and produced a stacked map showing either the probability of overcoming a given intensity measure of interest (e.g. for the ash fall), or the area covered by some specific scenarios of interest. On the other hand, index-based approaches look for combining the outputs of different hazard assessments defining indexes, mostly in a qualitative way, to somehow weight different features of the volcanic hazards as the frequency, intensity, spatial distribution, etc.; afterwards, the index values are combined or aggregated to identify hotspot areas that represent the zones subject to the impact of the different volcanic hazards. Examples of applications using a similar index-based approach for volcanic multi-hazard can be found, among others, in Thierry et al. (2008) for Mount Cameroon (Cameroon), Totaro et al. (2020) for the Neapolitan area (southern Italy), and Gjerløw et al. (2022) for the Jan Mayen Island (North-Atlantic).

The objective of these studies relies on the identification of hotspot areas that are potentially subject to multiple hazards, with the aim to support decision-making processes and emergency management, as well as for territorial planning. However, the amount and degree of subjective choices supporting most of the presented

studies (particularly those that are index-based) suggest that such approaches should be used with caution when communicating with authorities and for their effective use for specific purposes, e.g. civil protection.

Etna, which is one of the most active volcanoes on Earth, is characterized by frequent effusive and explosive eruptions occurring during a complex eruptive history over the last 500 ka. Lava flows, mostly those propagating from flank vents, have typically been considered the main hazard because they occur closer to vulnerable areas and, although they do not normally result in the loss of human lives, they can invade cultivated land and destroy human property and infrastructures (Coltelli et al., 2012; Branca et al., 2017; Centorrino et al., 2021). Explosive activity, characterized by ash dispersal and tephra fallout, strongly impacts the local economy, causing damages to infrastructures, agriculture and air traffic (Andronico et al., 2008). These volcanic hazards have been often accompanied by pre-, syn- and post-eruptive seismicity, suggesting possible correlations between seismic activity in nearby faults and the unrest of the volcano (Bevilacqua et al., 2022). Therefore, local communities living on the Etna's slopes are subject to huge inconvenience and economic losses, due to the simultaneous or sequential occurrence of these hazardous events linked to the eruptive activity of the volcano.

In this paper, we present a fully probabilistic approach, that we call 'target-based,' for MHA in which the outcome of harmonized single-hazard assessments are integrated following a transparent and clear logical pattern, and where the decisions regarding the specific choices for setting the quantitative analyses are objectively defined. Our MHA has currently been focused on the integration of different independent hazards in volcanic contexts, neglecting possible cascading effects.

The paper is structured as follows: first, we introduce the target-based approach for integrating the assessment of multiple independent hazards; second, we present a case study related to the assessment of different volcanic hazards in the municipality of Milo, located in the eastern flank of Etna volcano; third, we introduce an implementation example by defining a fault tree based on a specific scenario of interest for the decision-making process and showing the evaluation results.

2. Material and Methods

Probabilistic hazard assessment aims at quantifying the probability (or the rate) of exceeding a given intensity measure threshold (where the intensity measure is the physical parameter used to characterize the hazard) at a given spatial point and in a given exposure time of interest. For example, a probabilistic hazard for lahar may aim at assessing the rate of exceeding a specific threshold in the lahar thickness (the intensity measure) at a given point over the next, e.g. 50 years (the exposure time window). The results of such analysis are usually presented using the so-called hazard curves (for a vector of intensity threshold values), which describe the exceedance probability (or exceedance rate) as a function of increasing values of the intensity measure, at the point of interest and for the selected exposure time interval. If hazard curves are provided for different points covering a target area, it is possible to spatially represent on a map the probability of exceeding a specific intensity measure threshold or, conversely, the intensity measure value that has a specific exceedance probability or rate (Tonini et al., 2015). Examples of volcanic hazard assessments following this kind of approach are e.g. Biass et al. (2016) and Selva et al. (2018) for tephra fall, Martinez et al. (2022) for airborne volcanic ash, Sandri et al. (2024) for syn-eruptive lahars.

When analyzing different volcanic hazards, it is worth noting that the physical processes characterizing the hazard and the propagation of the intensity measure can be very different among them, making a direct comparison among them difficult. For example, while the intensity measure characterizing volcanic tephra fall is generally the thickness of the deposit (Connor et al., 2001) or its ground load (Biass et al., 2016), the volcano-seismic hazard can be characterized in terms of ground-motion parameters (as peak ground velocity, acceleration or displacement) or macro-seismic intensity (e.g. European Macroseismic Scale EMS-98, Grünthal, 1998), the lava flow hazard can be assessed using a binary criteria (reach/no reach a given point, Bilotta et al., 2023; Zuccarello et al., 2023).

From a decision-making point of view, a direct comparison of the output of different probabilistic hazard assessments may be confusing and lacking informativeness; however, as generally done in multi-risk analyses, a direct comparison or integration can be done when the multi-hazard assessment is then used for quantifying the potential impact or the risk (e.g. Marzocchi et al., 2012; Liu et al., 2015); indeed, the risk provides a metric to quantify the expected effects of the hazards, and it is such metric that is common to all the hazards.

Specifically for multi-hazard analysis, the amount of information that is contained in the hazard curves is very high, and we argue that such information can be used in a more appropriate way beyond the simple overlapping of

maps or definition of indexes. To support this argument, here we introduce a target-based approach in which the results of probabilistic single-hazard assessments are harmoniously and homogeneously integrated by introducing a tangible objective to the analysis (that we call a target objective) in a way that, without reaching a full risk analysis, it can properly support the decision-making process.

2.1 Target-based approach for volcanic multi-hazard analysis

Regardless of what the (volcanic) hazard source is, what is the probability that a hazardous event reaches an intensity value so that a pre-established target objective becomes true? This is the basic research question that the target-based MHA aims to answer. A target objective, TO, is defined as *a situation of interest to be assessed while considering the potential effects of different hazards in a given area*. The target-based MHA relies on the quantification of the probability that TO occurs as a consequence of the occurrence of one or more identified hazards. In the proposed method, the probabilistic analysis is performed using a fault-tree approach, which together with event trees, constitute the ground for the bow tie technique (e.g. Bedford and Cooke, 2001; Rausand and Høyland, 2004) that is widely used to analyze the interaction between different hazards and the potential consequences of domino effects (Garcia-Aristizabal et al., 2019; Gasparini and Garcia-Aristizabal, 2014).

In general terms, to implement a target-based MHA, it is necessary to clearly define: i) the TO of the analysis (TO setting and description); ii) the hazard identification and logical relationships among hazards (with respect to the defined TO); iii) a probabilistic single-hazard assessment; iv) a set of the hazard critical thresholds (with respect to the defined TO); and v) the fault-tree for linking and setting the MH analysis.

2.1.1 TO setting and description

Identifying and setting TOs is by far a simpler task for decision makers, since these objectives are tangible and, as described in the following paragraphs, their definition and setting choices are a fully transparent process. In our opinion, this is what gives it an edge over other approaches, such as the index-based one.

TOs that can be used for a target-based MHA are situations that define a tangible perturbation of a given nature and that a decision maker can identify as a potential problem triggered by one or more hazardous events in a given area; examples of such a kind of perturbation are, among many others, a given level of loss of functionality of a facility or infrastructure, significant impact on cultivated areas, etc.

2.1.2 Hazard identification and logical relationships among hazards

Identifying the hazards of interest is a key step for the target-based assessment; it implies selecting the hazardous phenomena that are specifically relevant for the defined TO. Moreover, it requires the setting of the logical relationships among hazards, that is, identifying how the different hazards can concur to reach the effect defined by the TO. As example, let's look at a hypothetical case in which the analysis involves three hazards, H_1, H_2, and H_3; according to the TO and how these hazards may contribute to reach the TO, a decision maker could set the following logic relationships for a given TO:

- H_1 or H_2 or H_3: i.e. the occurrence of any one of the input hazards will cause the TO to occur.
- [H_1 and H_2] or H_3: i.e. TO occurs if both [H_1 and H_2] occur or only H_3.

Such simple examples illustrate the different scenarios that can be defined and assessed using this approach; such logical relationships constitute the scenarios that will be implemented in the fault tree for the quantitative analysis, as shown in Section 2.1.5.

2.1.3 Probabilistic single-hazard assessment

Fully-probabilistic hazard assessment (PHA) is required for each of the different hazards identified for the target-based MHA. The key element for the PHA of the different hazards is their homogeneity, that is, they should be assessed over the same target area, as well as over the same exposure time window.

The specific methods for the assessment of each hazard pertain to each scientific community dealing with the specific hazard; as a result, the PHA must be performed producing a hazard curve at each point $x^{\rightarrow}$ of the target area; as already mentioned, the hazard curve represents the probability $\Pr\{IM \geq im_t;\ \vec{x};\ \Delta t\}$, where IM is the intensity measure characterizing a specific hazard, im_t a vector of threshold values of the intensity measure, $\vec{x}$ the point in the target area, and Δt the exposure time window used in the analysis.

2.1.4 Setting of the critical intensity thresholds

The hazards identified for the analysis represent events whose occurrence, above a critical intensity threshold (specific for each hazard), is likely to cause the occurrence of TO. The critical intensity thresholds, im_t, are therefore a set of hazard-specific IM values that the decision maker takes into account as the limit values of the various hazard intensities above which the undesired outcomes, set by the TO, may be true. Defining the critical thresholds is one of the most important decisions that the MH analyst needs to take; in the most objective assessment, they can be set using 'impact' or 'effect' functions (as e.g. damage curves, fragility functions, etc., defined according to the elements considered in the TO) which provide the probability *Pr{impact|IM}* of reaching the defined impact D conditional on the value of the intensity measure considered for the hazard. In the most general applications, the critical thresholds can be set high enough so that one can realistically assume that $\Pr\{impact \mid im_c\} \approx 1$.

2.1.5 Fault-tree setting and analysis

The quantitative evaluation of the Fault-trees for MH assessment has been performed using the tool developed by Garcia-Aristizabal et al. (2019), which is freely available in the EPOS (European Plate Observing System) infrastructure of the Thematic Cor Services "Anthropogenic Hazards" (available at the site: https://tcs.ah-epos.eu/episodes/, adapting it to assess fault-trees in a dense grid of target points; see Garcia-Aristizabal et al., 2019; Orlecka-Sikora et al., 2020). A fault tree is a graphical representation of the logical relationships of basic events that lead to the occurrence of the undesirable critical situation defined as the top event (Bedford et al., 2001). In our implementation, the top event corresponds to the TO; once the TO is defined, all possible ways for the TO to occur are systematically deduced until the required level of detail is reached (Garcia-Aristizabal et al., 2019). Events whose causes have been further developed are intermediate events, and events that terminate branches are basic events (BE). The fault tree implementation is based on three assumptions: (1) events are binary events (do occur/do not occur); (2) basic events are statistically independent; and (3 relationships between events are represented by means of logical Boolean gates (mainly AND, OR). The probability of occurrence of the TO is therefore calculated from the occurrence probabilities of the BEs.

The target-based MHA using a fault tree approach can be straightforwardly implemented when analyzing hazards related with different sources (e.g. volcanic, climate-related, tectonic, etc.). However, when analyzing different volcanic hazards related to the activity from the same volcano, as in this work, a common cause effect can mine the assumption of independence for identifying the BEs; in such cases, the assumption of independence requires careful consideration in order to avoid significant biases. In general, natural hazards may appear independent at first glance, but can have underlying dependencies due to shared root causes, physical processes, or geographic correlations. If available, historical data can be used to assess the likelihood that joint occurrences are statistically significant.

Possible dependencies can be accounted for either through conservative assumptions or by quantifying them using past data or combined event modelling.

The BEs are the root causes leading to eventual intermediate events and, ultimately, the top event (i.e. our TO). These are typically the lowest level in the fault tree, and therefore they are the events where the probabilistic analysis is focused. In our approach, the BEs correspond with the identified hazards for the MHA; once a fault tree has been defined and the critical intensity measures have been set, we use the output of the single PHAs to define the parameters of the BEs of the fault tree. In practice, for the i-th hazard H_i related to the BE_i of the fault tree, we *cut* the hazard curve of the point $\vec{x}$ to extract the probability of exceeding im_c. If a quantification of the uncertainties (e.g. epistemic uncertainties) is available, i.e. if a set of hazard curves has been estimated representing the different percentiles of the hazard (Tonini et al., 2015), the set of hazard curves will be cut to achieve a distribution of the probability of exceeding im_c, and then a sample from that distribution will be extracted.

To model the stochastic features of the BEs, Garcia-Aristizabal et al. (2019) use a number of probabilistic models using Bayesian data analysis techniques. It is worth noting that while the use of a Bayesian approach is not necessary for the probabilistic assessment of the BEs, we believe that adopting such an approach provides a number of advantages, allowing us to integrate different sources of information (e.g. from physical modeling and form field observations) and to directly deal with epistemic uncertainties that are ubiquitous in natural hazards. For this reason, in this paper we adopt the Bayesian implementation, proposing to encode the output of hazard assessments based on physical modelling as a prior state of information, and to use other data eventually available (as e.g. field observations, data from past events, etc.) to set a likelihood function to update the prior state of information.

For the application presented in this paper, the following two classes of probabilistic models for implementing the stochastic characteristics of fault-tree's BEs can be of interest: the Homogeneous Poisson model and the Binomial model. As already stated in the previous paragraph, the advantage of the Bayesian implementation is the opportunity to set a prior state of knowledge and to define a likelihood function using site-specific data for each BE of the FT; nevertheless, the general approach of using a FT technique for the MHA can be implemented avoiding the Bayesian formalism setting a distribution characterizing the probability of each BE.

In this section, we briefly indicate the main features of the implemented models, as well as the input/output parameters required for defining a given BE according to these models. A detailed description of the mathematical background is presented in Garcia-Aristizabal et al. (2019).

2.1.6 Homogeneous Poisson process (HPP)

In this case, the inference problem is to estimate the rate (λ) at which a given intensity measure value is exceeded per time unit. For simplicity, we adopt the conjugate pair Poisson likelihood / Gamma prior (Gelman et al., 1995), which is one of the most frequent models used in risk assessment applications (Siu and Kelly, 1998).

The prior distribution for λ can be developed from the outcome of hazard simulations or, if not available, from other sources expert opinion elicitation. Because of the simplicity in calculations, we adopt a conjugate prior for the λ parameter, which in this case is the Gamma distribution:

$$\pi_0(\lambda) = \frac{\beta^\alpha \lambda^{\alpha-1}}{\Gamma(\alpha)} e^{-\beta\lambda} \tag{1}$$

Where α and β are the parameters characterizing this distribution. To define the prior model parameters from hazard curves we can estimate mean rate, **E(λ)**, as a best value, whereas a standard deviation, **SD(λ)** can be derived from eventual epistemic uncertainties associated with the hazard assessment. In such a case, the α and β parameters of the Gamma prior distribution can be set by solving (e.g. Garcia-Aristizabal et al., 2019):

$$\begin{cases} E(\lambda) &= \dfrac{\alpha}{\beta} \\ \mathrm{SD}(\lambda) &= \dfrac{\sqrt{\alpha}}{\beta} \end{cases} \tag{2}$$

The (Poisson) likelihood function is set for encoding the site-specific data which, for a HPP is basically the number ***r*** of events for which the critical threshold has been actually exceeded in a given point of the domain in a time interval $\Delta t = [0,t]$. The likelihood function for this evidence can be set using the Poisson distribution:

$$p\{r \text{ critical im exceedances}[0,t]|\lambda\} = \frac{(\lambda t)^r}{r!} e^{-\lambda t} \tag{3}$$

Table 1 summarizes the data required for defining a basic event as a homogeneous Poisson process. The Posterior distribution, π(λ), for the Poisson-Gamma conjugate pair is the Gamma distribution:

$$\pi_1(\lambda|E) = \frac{\beta'^{\alpha'}\lambda^{\alpha'-1}}{\Gamma(\alpha')}e^{-\beta'\lambda} \tag{4}$$

where

$$\alpha' = \alpha + r \quad \text{and} \quad \beta' = \beta + t \tag{5}$$

Once the posterior distribution $\pi_1(\lambda|E)$ has been obtained, samples of λ are drawn from that posterior distribution, which afterwards are used to calculate the probability of at least one event occurring in a determined period of time Δt of interest:

$$Pr(r > 0, \Delta t) = 1 - e^{-(\lambda \Delta t)} \tag{6}$$

Element	Parameter	Description
Prior distribution	E(λ), [0 ≥ E(λ) ≥ 1]	Prior assumption for the mean value for the rate of event occurrences (lambda)
	SD(λ)	Standard deviation of the prior mean value
Likelihood function	r, ($r \geq 0$)	Number of events occurred in a time interval Δt
	Δt, ($\Delta t > 0$)	Observation time (in years)

Table 1. Parameters required for setting a basic event of class HPP.

3. Case study

To demonstrate the performance of the proposed approach, we provide a worked example for multi-hazard assessment in the area of Milo municipality, located in the eastern flanks of Etna volcano. The eastern flanks of Etna volcano have been frequently affected by volcanic hazards from Etna volcano (among others, see e.g. Branca and Abate, 2017; Azzaro and Barbano, 1996); Milo is a small village that lies at an average altitude of 750 m a.s.l., it has a population of about 1,100 inhabitants, and due to its location (about 13 km, in a beeline), it has been frequently affected by Etna volcanic activity (as e.g. tephra fall, Mereu et al., 2024). Probabilistic volcanic hazards at Etna volcano have been recently assessed in the framework of the INGV project "Pianeta Dinamico – PANACEA" (Probabilistic Assessment of volcano-related multi-hazard and multi-risk at Mount Etna), funded by the Italian Ministero dell'Università e della Ricerca (MIUR, now "Ministero dell'Istruzione e del Merito"), which aimed at implementing multi-hazard and multi-risk assessments considering volcanic hazards at Etna.

As discussed in Section 2.1.5, analyzing together volcanic hazards from the same volcano can lead to potential biases in the FT assessment due to a common cause effect. Combined event modelling could be the best way to evaluate the effect of spatial and temporal correlation of the analyzed hazards, but taking into account the number of required simulations and the computational cost for modeling some hazards (in particular lava flows and tephra dispersion), this possibility is currently unfeasible. Nevertheless, we argue that, given the hazards analyzed in this paper (seismic, tephra fall, and lava flooding), the potential effect of common causes can be assumed negligible after taking into account different observations.

First, regarding the seismic hazard, most of the seismic events used to produce the hazard map are not always directly linked to Etna's volcanic eruptions (see e.g. Bevilacqua et al., 2022); indeed, these authors have assessed the possible correlation between large seismic events (the more relevant events for the hazard) and the occurrence of eruptive activity, finding in some cases an increase in the probability of earthquakes occurring in a time window after the occurrence of flank eruptions (Bevilacqua et al., 2022). Moreover, even in such cases, while the flank eruptions take place in the volcanic edifice, seismic events are associated to distal faulting systems and the spatial distribution of peak ground motions and the eruptive vent opening (potential source for lava and tephra) are in any case not necessarily correlated.

Second, the hazards from lava flows and tephra load from a flank eruption may be actually linked to the occurrence of the same eruptive event (i.e. a flank eruption with effusive and explosive phases, which have actually happened at Etna, for example in 2002-2003). However, whereas the hazard from lava flows reaching Milo town (that is, the target area in this study) is due to a very small fraction of all the possible flank eruptions that could open on the wide edifice of Etna volcano, the hazard from tephra is basically posed by almost any flank eruption with an explosive phase, due to the prevailing winds in the target area and the relative position of Etna volcanic edifice and Milo town. In other words, only a very small fraction of all the possible flank eruption would concur to the hazard both in terms of tephra load and lava flow invasion. We acknowledge this is not a completely sound reason, but given the illustrative nature of the example and the prevalence of tephra load and seismic hazards with respect to the one for lava flow invasion, we assume that neglecting this dependency in the final computation can be considered a safe assumption. Unfortunately, we currently do not have sufficient information and capability to run combined simulations of flank eruptions with effusive and explosive phases to assess both hazards simultaneously and, therefore, explicitly taking into account the potential dependency. In light of all the considerations just made, we move forward assessing each single hazard independently.

3.1 Target objective definition

To define a TO, in this work we assume a possible scenario of interest that a decision maker could be interested in. We assume that the decision maker is interested in considering as TO *eventual disruptions caused by volcanic hazards on any element of the road network* in an area of competence of Milo municipality, Sicily.

To build this example scenario, we assume that the hazards that are relevant for assessing the TO of interest for the decision maker are the lava flow, the tephra fall, and the seismic ground motions, and that the effects defined in the TO are reached when the intensity measures of these hazards reach the critical intensity measure thresholds defined in Table 2. The choice of the im_c is a task that is intrinsically linked to the TO and, therefore, to the specific interest of the decision maker for the analysis. For example, the thresholds defined for the TO considered in this case study could be derived from assuming hazard levels having the potential of disrupting the functionality of the road network, as for example: (i) a thickness of tephra that significantly increases the risk for vehicles to use the road, (ii) a lava flow reaching the road with the potential of blocking it, and (iii) a level of ground motion intensity with the potential of blocking road circulation due to many factors as partial collapses in the built environment (whose debris deposits can block the road), triggering landslides, or effects on bridges that may induce to stop transit for checking the integrity of the structure.

The next step consists in defining how the occurrence of these events can contribute to reaching the TO, which is necessary to define logical operations for constructing the fault tree for assessing the probability of occurrence of the TO. In this example, we assume that any one of the three hazards taken alone is capable of making the TO defined in this case study true; therefore, the logical combination of basic events can be built combining all the hazards using OR gates, resulting in a fault tree as the one shown in Fig. 2 (second row of events under the blue OR gate). It means that we expect that the effects described by the specific TO under analysis can be reached when any of the considered hazards reach or overcome the defined critical threshold. Finally, regarding each single hazard, the probability that each specific hazard produces the effects described by the TO can be calculated considering the combination of the probability of overcoming its specific critical im_c and the probability that an intensity greater or equal to im_c actually causes the expected effects; this calculation can be done using an AND gate, as shown in the bottom events of Fig. 2. While the first term is actually the result of the hazard assessment (Section 3.2), the second one, if required, can be calculated based on vulnerability assessments of the target objective defined for the analysis.

Keeping in mind the specific TO defined in this work, we assume that the selected im_c are high enough in order to assume that the second term is near to one.

Hazaård	Definition of critical intensity measure	
	Intensity measure parameter	im_c
Lava inundation	h_L (thickness, m)	$h_L > 0$
Tephra fall	h_T (thickness, m)	$h_T > 0.05$
Seismic hazard	Macroseismic intensity (EMS scale)	VII

Table 2. Critical intensity measure (im_c) thresholds selected forthe case study in Milo municipality (Sicily) for assessing the scenario for the TO defined by a hypothetical decision maker (TO: disruptions caused by volcanic hazards on any element of the road network).

3.2 Independent, single hazard assessment

The probabilistic hazard assessment for the lava inundation, the tephra fall, and the seismic ground motions have been performed in the framework of the INGV's project Pianeta Dinamico (PANACEA), and the results of these hazard assessments are published in this special issue. In the following paragraphs we provide the references and briefly describe the approaches used for the single hazard assessments and the data used for the present case study.

The lava flow hazard was assessed using the new methodology presented in Cappello et al. (this issue). The hazard map was computed by performing lava flow simulations using the physics-based GPUFLOW model (Cappello et al., 2022) on a Digital Surface Model obtained from Pleiades imagery acquired on 9 July 2019 (Ganci et al., 2023). The numerical simulations were performed on a 20 m grid and the output of these simulations, combined with the probability of vent opening (Sandri et al., 2024), was used to calculate the probability of lava flow inundation. For this case study, the hazard information (i.e. the probability of lava flows reaching a given point in 10 years) was extracted from the grid points located in the area of Milo municipality, from where we calculated the annual exceedance rates (Fig. 2a).

The methodology used for the tephra hazard assessment is presented in Scollo et al. (this issue). Due to the exposure time considered (10 years), we focus only the hazard from the tephra accumulated at the ground during flank eruptions, neglecting summit eruptions. For flank eruptions, Scollo et al. (this issue) simulated tephra dispersion using the TEPHRA2 model and accounting for the spatial probability of vent opening on the flanks of Etna (Sandri et al., 2024), for the altitude of the vent and the surrounding topography, and a statistics of wind fields extracted from the ECMWF ERA5 reanalysis database (Hersbach et al., 2018) over the period 2007-2019. The results of these simulations were processed to obtain hazard curves on a 500 m grid covering eastern Sicily to Calabria. For this study, we used the hazard curves from the grid points located in the Milo municipality, extracting the probability of exceeding 5 cm of tephra thickness in 10 years, and from where we calculated the annual exceedance rates, as shown in Fig. 1b.

The probabilistic seismic hazard assessment (PSHA) refers to the local volcano-tectonic seismicity and is aimed at assessing the hazard for short exposure times (5, 10 and 30 years, D'Amico et al., this issue). The analyses are performed using the code SASHA (D'Amico and Albarello, 2008) which makes use of the observed macroseismic data taken from the Catalogo Macrosismico dei Terremoti Etnei (CMTE, Azzaro and D'Amico, 2014) to compute the macroseismic history for each investigated locality, and integrates "virtual" intensity values calculated according to attenuation laws specifically developed for volcanic areas (Rotondi et al., 2016). The results (see D'Amico et al., this issue) are calculated on a 500 m resolution grid and are given both as macroseismic intensity (EMS-98), as well as peak ground acceleration (PGA) for a chosen exceeding probability threshold. For this case study, we used the hazard curves from the grid points located in the Milo municipality, as shown in Fig. 1c, from which we extracted the probability of exceeding the VII intensity in 10 years that are then used to calculate the annual exceedance rates.

(a)

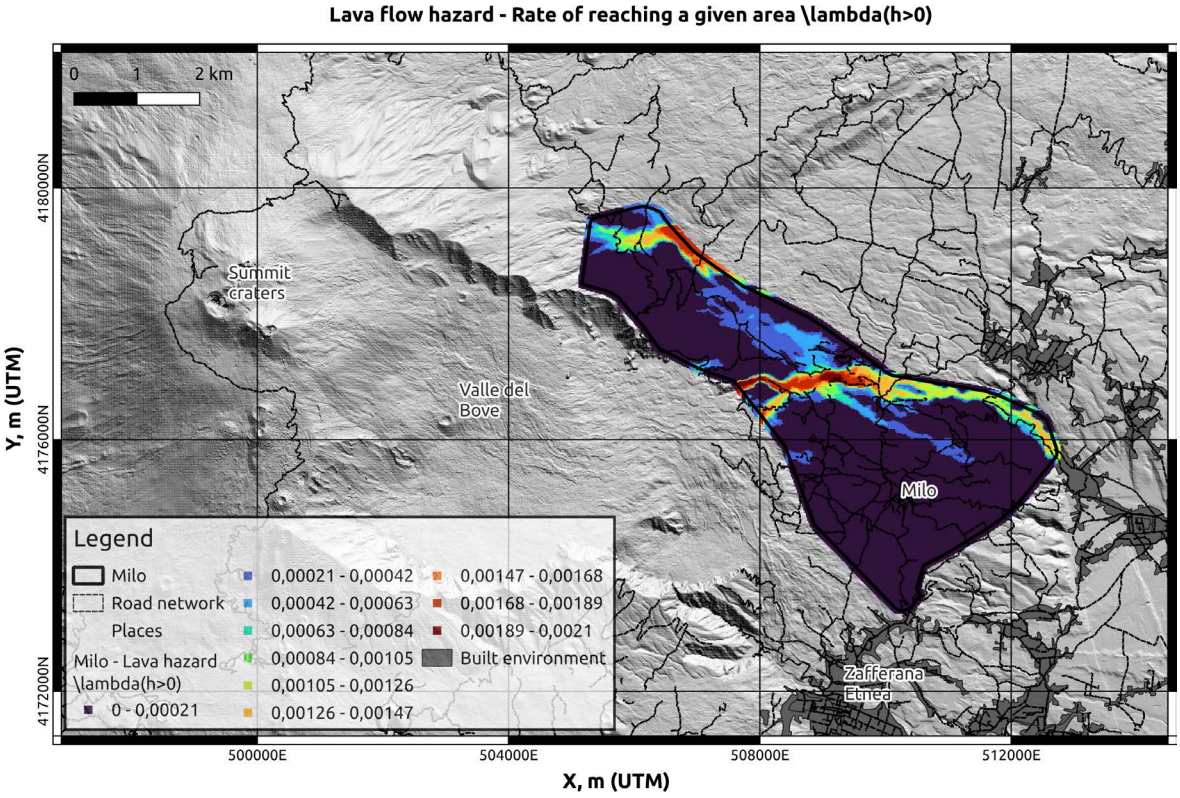
Lava flow hazard - Rate of reaching a given area \lambda(h>0)
0 1 2 km
Summit craters
Valle del Bove
Milo
Zafferana Etnea
Legend
Milo
Road network
Places
Milo - Lava hazard \lambda(h>0)
0 - 0,00021
0,00021 - 0,00042
0,00042 - 0,00063
0,00063 - 0,00084
0,00084 - 0,00105
0,00105 - 0,00126
0,00126 - 0,00147
0,00147 - 0,00168
0,00168 - 0,00189
0,00189 - 0,0021
Built environment
4180000N
4176000N
4172000N
500000E
504000E
508000E
512000E
Y, m (UTM)
X, m (UTM)

(b)

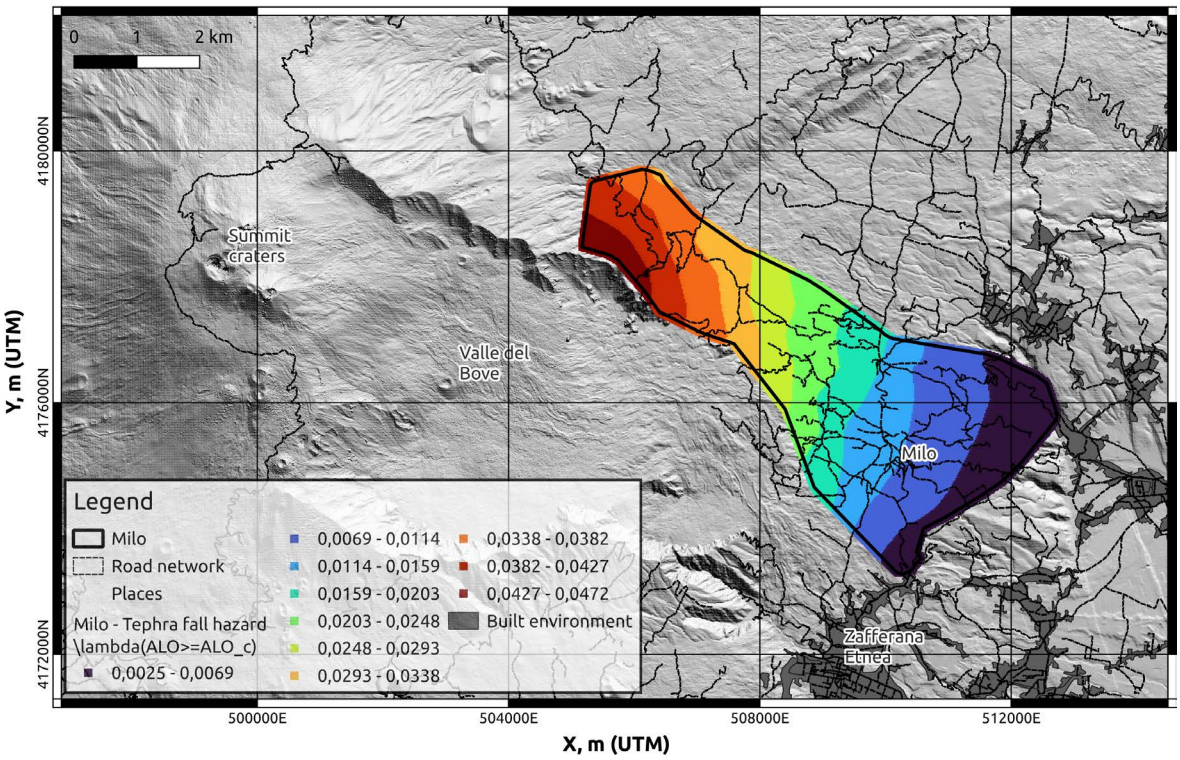
Tephra fall hazard - rate of exceeding a critical intensity measure (ash load)
0 1 2 km
Summit craters
Valle del Bove
Milo
Zafferana Etnea
Legend
Milo
Road network
Places
Milo - Tephra fall hazard \lambda(ALO>=ALO_c)
0,0025 - 0,0069
0,0069 - 0,0114
0,0114 - 0,0159
0,0159 - 0,0203
0,0203 - 0,0248
0,0248 - 0,0293
0,0293 - 0,0338
0,0338 - 0,0382
0,0382 - 0,0427
0,0427 - 0,0472
Built environment
4180000N
4176000N
4172000N
500000E
504000E
508000E
512000E
Y, m (UTM)
X, m (UTM)

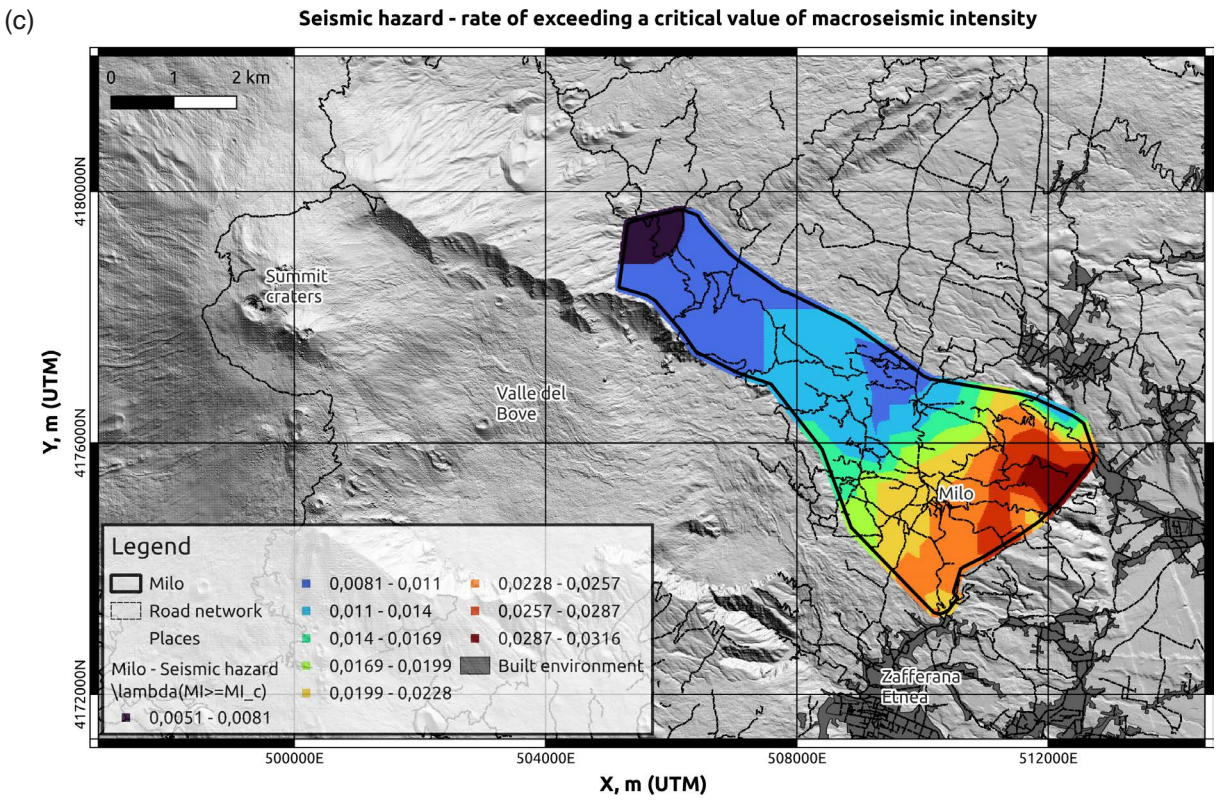

Figure 1. Single hazards: (a) lava flow (annual rate of lava reaching each point of the spatial domain), from Cappello et al. (2025); (b) Tephra fall (annual rate of exceeding 5 cm of ash thickness), from Scollo et al. (2025); (c) Volcano-seismic hazard (annual rate of exceedance of a macroseismic intensity of VII, approximately corresponding to a PGA of ~1.7 ms^{-2}), from D'Amico et al. (2025). The results are shown in a harmonized spatial grid.

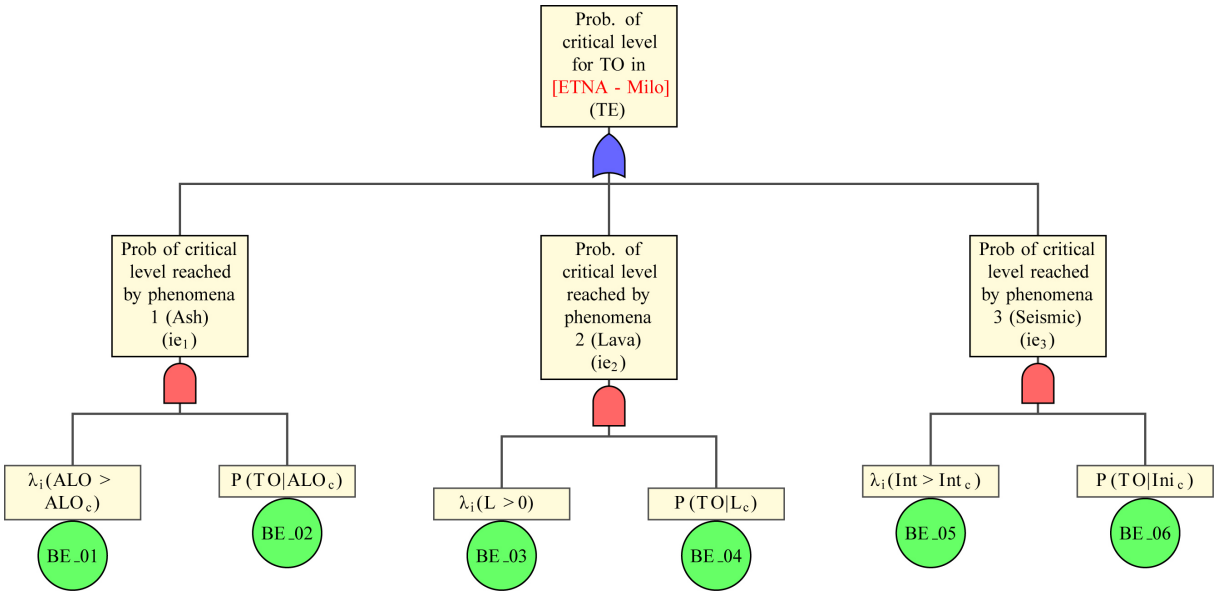

Figure 2. Fault tree defined for MH analysis considering three hazards (lava flow, tephra fall, and seismic hazards). The fault tree was built in order to assess the probability of a specific TO defined as "*eventual disruptions caused by volcanic hazards on any element of the road network*" in the Milo municipality near Etna volcano.

4. Results

As described in Section 3, single hazard assessments for lava invasion, seismic ground motions, and tephra fall were assessed using different spatial resolutions. At each grid point of the spatial domain, a full hazard curve, providing the probability of reaching or exceeding different IM values, is available; moreover, epistemic uncertainties were assessed for the lava and the tephra fall hazards. The first step in the analysis was to extract, for each hazard, the probability of exceeding the critical intensity measure (im_c) in a time window Δt along with the uncertainty range in the hazard estimation (if available) and used this information to calculate the annual exceedance rates (assuming a poissonian process in the time domain). The im_c used for the case study are summarized in Table 2.

Afterwards, we harmonized the spatial resolution of the different hazards by downscaling both the tephra and the seismic hazard rate values in order to obtain values at the same spatial resolution of the lava hazard probabilities (20 m grid); the downscaling was performed using spatial bilinear interpolation among grid points. In this way, we obtained exceedance rates of the im_c values for the three hazards in a common spatial grid, which for the study area is composed of 42431 nodes (Figs. 1a, 1b and 1c).

After reaching the spatially harmonized hazard information, at each node of the domain we encoded the hazard information as a BE of the FT shown in Fig. 2 using the Homogeneous Poisson model (Section 2.1.6). In practice, the outcome of the model-based hazard assessments described in Section 3.2 were used to set the prior state of information for the rate parameter (λ) of the Poisson process using the Gamma distribution (Eq. 1). The α and β parameters of the Gamma distribution are set using the mean and the standard deviation of λ inferred from the epistemic uncertainty information, solving the system of equations shown in Eq. (2). For the seismic hazard, which does not provide an uncertainty estimate of the hazard assessment, we assumed a standard error of the estimated value as $\sim\sqrt{\lambda}$.

Once the prior state of knowledge for the rate of threshold exceedances (Eq. 1) has been defined, eventual observations of past event in given areas can be taken into account by setting the Poisson likelihood function; with this aim, at each place of interest it is possible to count the number of times that the im_c threshold has been exceeded in a given area and in a determined time interval ($\boldsymbol{r}$, and Δt, see Eq. 3). Using this information, the posterior probability density for the λ parameter can be calculated (Eqs. 4 and 5). Figure 3 shows an example of the prior and posterior PDF for λ one of the nodes randomly selected in the analyzed domain (UTM coordinates X = 4173320 m, Y = 510220 m); the plot in Fig. 3a corresponds with the Gamma prior and Gamma posterior distribution considering the data obtained from the seismic hazard in the selected place, and where $E(\lambda) = 2.2 \times 10^{-2}$ (annual exceedance rate from the hazard model output), r = 0 (number of observed exceedances in Δt), and $\Delta t = 10$ yr.

Samples of λ are drawn from the posterior distribution defined at each node and, using Eq. (6), these values are used to calculate the probability of exceedance in Δt.

The fault-tree structure is then quantitatively assessed by using the probability data from the BEs. The fault tree is solved using Monte Carlo simulations as implemented in the approach presented in Garcia-Aristizabal et al. (2019) and freely available in the infrastructure of the European Plate Observing System (EPOS), thematic core services Anthropogenic hazards (accessible at the link: https://tcs.ah-epos.eu/). In practice, the FT is solved using Monte Carlo simulations by sampling the probability distributions defined for each BE; in this way, it is possible to obtain an empirical distribution for the probability of the top event of the FT which corresponds with the TO under analysis, as shown in Fig. 3b.

The empirical distribution obtained at each node for the probability of the top event of the fault tree provides information of the multi-hazard assessment for the TO under analysis; since the TO of the example presented in this paper is defined as "*eventual disruptions caused by volcanic hazards on any element of the road network*" in the Milo municipality, to represent the result in a map we extract the nodes located in the track of the road network and plot different percentiles of these empirical distributions. Figure 4 shows the results of the MH assessment considering the combined effect of the three hazards included in this example and according to the fault tree shown in Fig. 2; Figure 4a represents the median of the empirical distribution in all the nodes located in the road network in the study domain, whereas Figs. 4b and 4c show, respectively, the 16^{th} and 84^{th} percentiles of the distribution to represent uncertainty bounds for the MH estimate.

Comparing the probability values of each single hazard (Fig. 1) with the results of the MH analysis after combining them using the fault tree structure shown in Fig. 3, the probability of reaching the analyzed TO increases in about one order of magnitude respect to the highest single hazards, that in this example corresponds to the seismic and tephra fall. This result is directly linked to the logical relationship considered in the fault tree; linking all the hazards

(a)

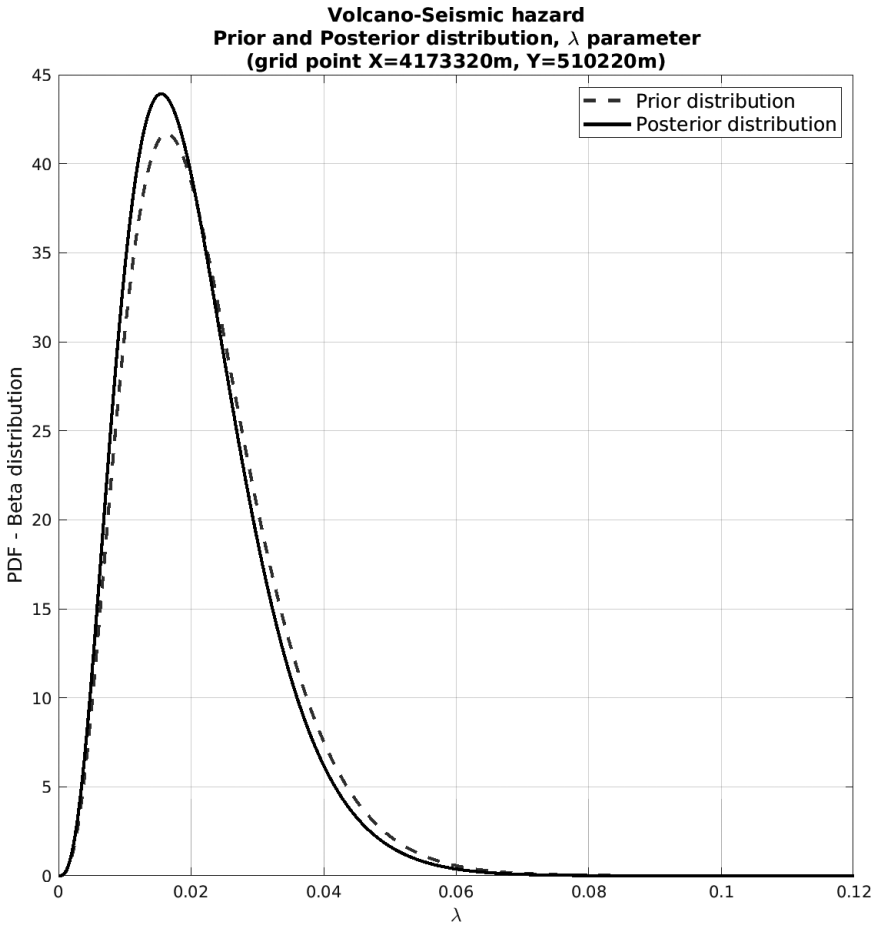

(b)

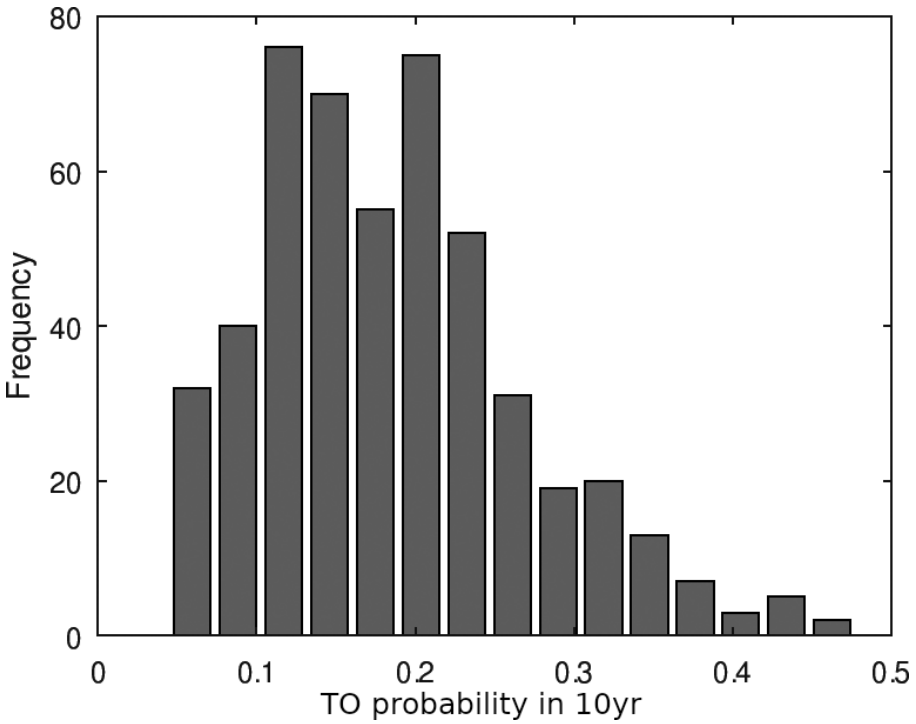

Figure 3. (a) Example of the Bayesian inference of the λ parameter of the Homogeneous Poisson model used to encode the seismic hazard in a sample node of the case study domain (UTM coordinates X = 4173320 m, Y = 510220 m). The plot shows both the prior and posterior distributions of λ in a sample grid point of the domain.(b) Empirical distribution for the probability in 10 years of the top event of the FT which corresponds with the TO under analysis in the same sample node (UTM coordinates X = 4173320 m, Y = 510220 m).

(a)

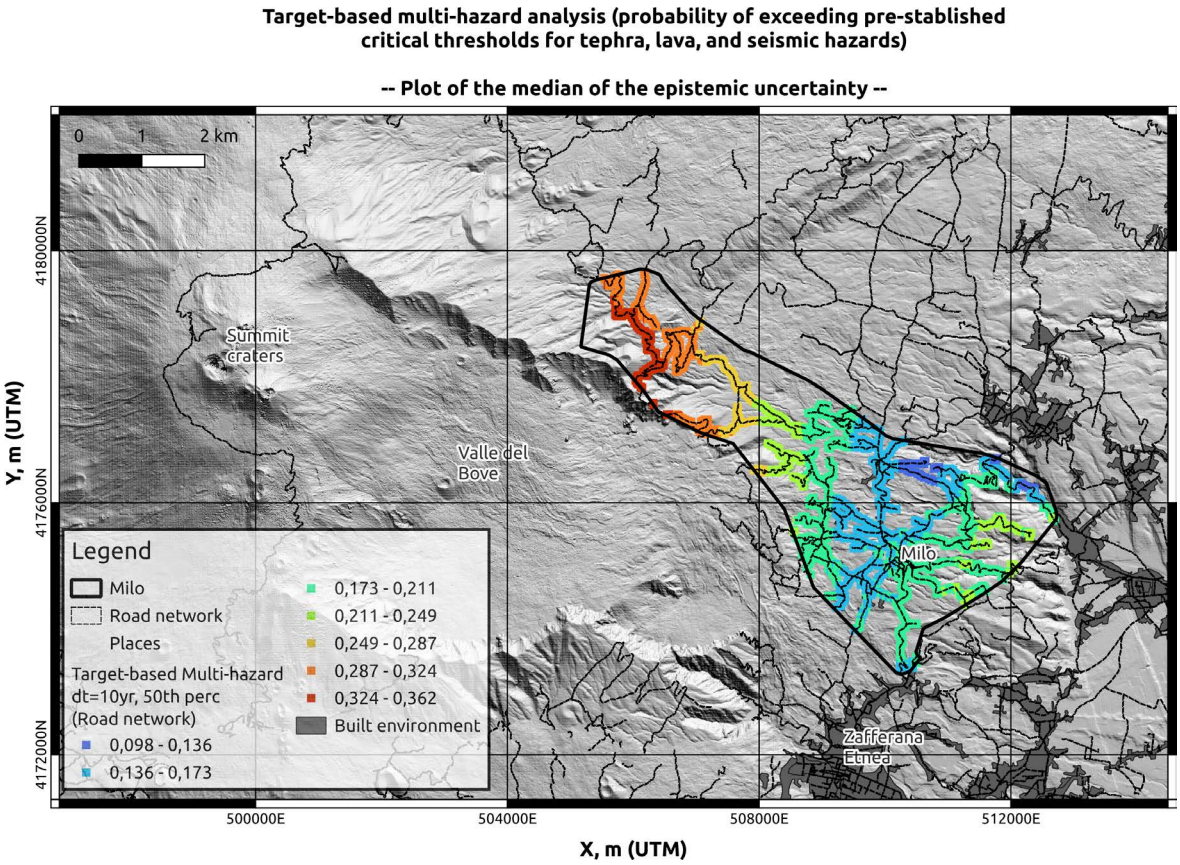
Target-based multi-hazard analysis (probability of exceeding pre-stablished critical thresholds for tephra, lava, and seismic hazards)
-- Plot of the median of the epistemic uncertainty --
0 1 2 km
Summit craters
Valle del Bove
Milo
Zafferana Etnea
Legend
Milo
Road network
Places
Target-based Multi-hazard dt=10yr, 50th perc (Road network)
0,098 - 0,136
0,136 - 0,173
0,173 - 0,211
0,211 - 0,249
0,249 - 0,287
0,287 - 0,324
0,324 - 0,362
Built environment
4180000N
4176000N
4172000N
500000E
504000E
508000E
512000E
Y, m (UTM)
X, m (UTM)

(b)

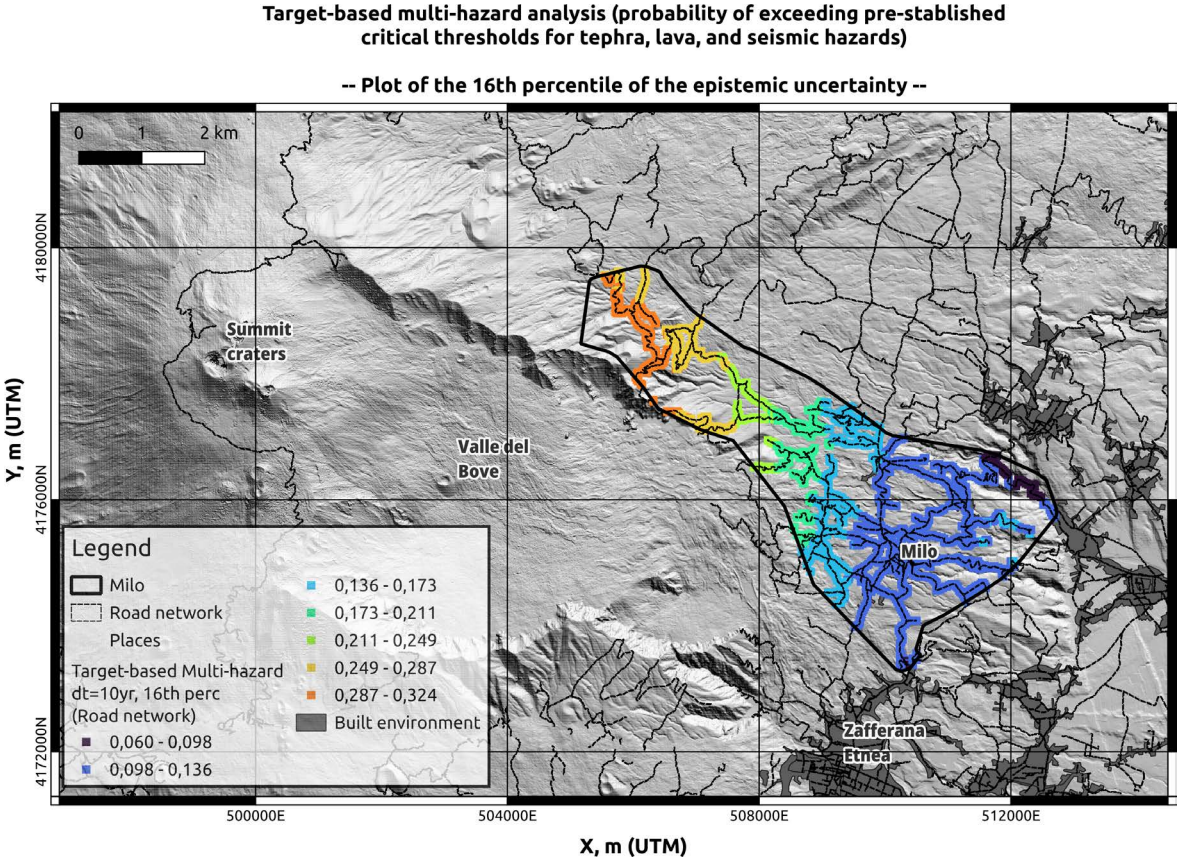
Target-based multi-hazard analysis (probability of exceeding pre-stablished critical thresholds for tephra, lava, and seismic hazards)
-- Plot of the 16th percentile of the epistemic uncertainty --
0 1 2 km
Summit craters
Valle del Bove
Milo
Zafferana Etnea
Legend
Milo
Road network
Places
Target-based Multi-hazard dt=10yr, 16th perc (Road network)
0,060 - 0,098
0,098 - 0,136
0,136 - 0,173
0,173 - 0,211
0,211 - 0,249
0,249 - 0,287
0,287 - 0,324
Built environment
4180000N
4176000N
4172000N
500000E
504000E
508000E
512000E
Y, m (UTM)
X, m (UTM)

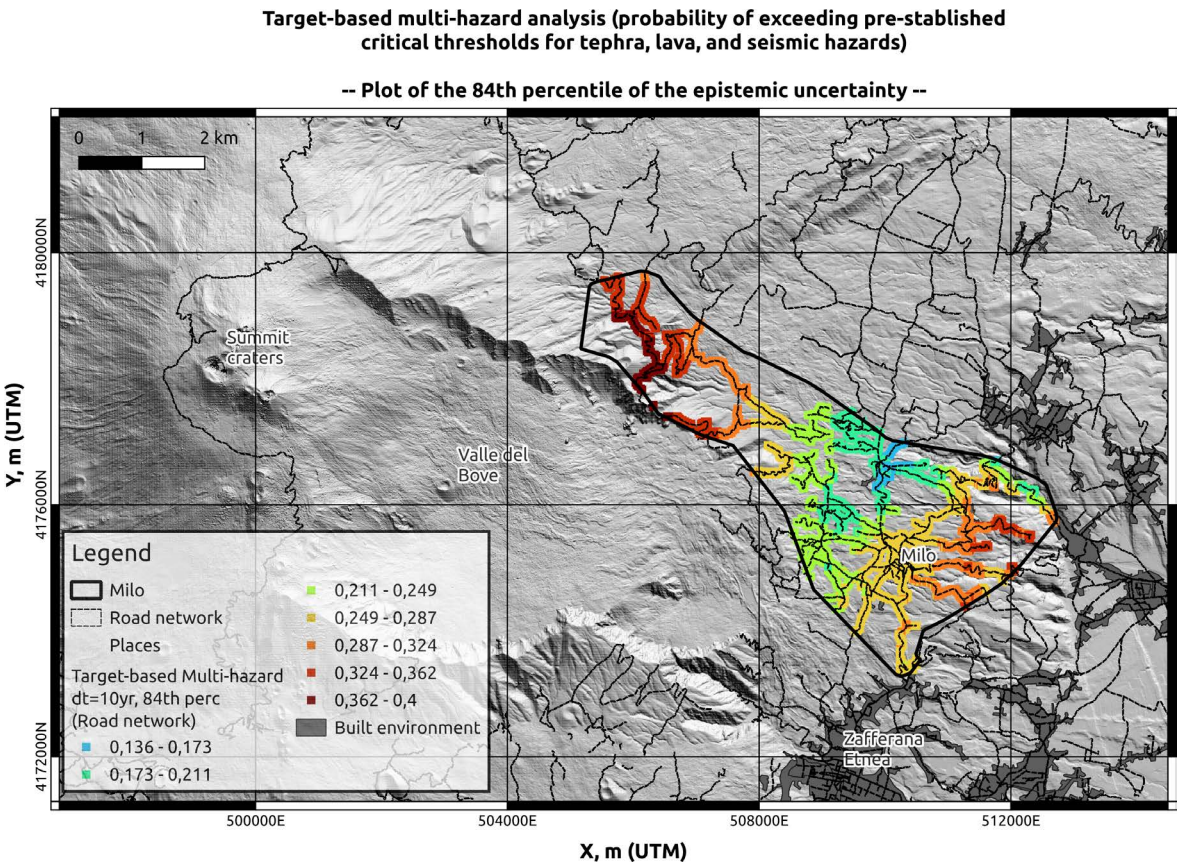

Figure 4. MH analysis showing the probability of the event defined in the TO as "*eventual disruptions caused by volcanic hazards on any element of the road network*" in the Milo municipality, on the south-east flank of Etna. (a) Median of the empirical distribution calculated in all the nodes located in the road network of Milo; (b) and (c) shown, respectively, the 16th and 84th percentiles of the empirical distribution as uncertainty bounds for the assessment. In all the plots, the values represent the probability of racing the TO in 10 years.

with an OR gate indicates that the output event will occur if at least one of the independent hazards occurs, making more likely the TO to become true (with respect to each single hazard taken alone). As can be seen in Fig. 4a, the highest combined hazard for the road network in Milo in this scenario corresponds, first, with regional roads in the upper E-NE flank of Etna, which is mostly due to the effect of tephra fall in this high-altitude zone of the volcano; the second largest effect is on the roads at the East of Milo where the main contribution comes from the seismic hazard.

5. Discussion

In this paper we present an approach for multi hazard analysis that has been designed to produce a tool to support decision makers for assessing, in an integrated way, the output of multiple single hazard assessments. The method assumes that single hazards have been assessed using state of the art probabilistic methods, in which hazard curves, representing the probability of overcoming different intensity levels (specific for each hazard), are available with a spatial and temporal resolution compatible with the objective of the multi-hazard analysis. In this regard, one of the main issues for implementing this approach is to harmonize in time and space the output of independent hazard assessments; therefore, a first step of hazard harmonization is required, ensuring that the exposition time for all the hazards is the same and, once the intensity thresholds are defined and the respective probabilities are extracted from the hazard curves, the values are downscaled to the same spatial grid which needs to be compatible with the objective of the analysis.

Once such technical issues are guaranteed, the results of single probabilistic hazards assessments can be used for assessing a wide set of scenarios according to the needs of decision makers; such scenarios can be built on

the basis of specific interests defined in the TOs, which can be set to explore different situations that can become true due to the effects of a number of single or multiple hazards. The way in which these hazards can be analyzed together is defined in the structure of a fault tree, in which the logical relationships of basic events that lead to the occurrence of the undesirable critical situation can be defined. It is worth noting that the use of the FT approach assumes that BEs are independent events; as described in the previous sections, it is necessary to evaluate possible correlations between hazards, especially between different volcanic hazards of the same volcano, to minimize the risk of biases due to common cause effects.

The vision of this approach consists in providing a tool for decision makers in which the output of probabilistic hazard assessments can be straightforwardly used in a practical and tangible way. The key elements for the analysis are (i) the definition of one or more TO in a clear way, (ii) the identification of the hazards and the way in which such hazards can contribute in reaching the TO, and (iii) defining the critical intensity thresholds for each hazard as values that are relevant for the TO becoming true. As can be seen, defining these three elements is a relatively simple and intuitive task, which makes it relatively easy to set up a MH analysis.

Setting the TO, hazards of interest and critical thresholds can be driven by specific and detailed interests, as e.g. when considering punctual critical infrastructures, or by generic settings for exploratory analysis; in this way multiple MH maps, related to a virtually large number of different scenarios, can be assessed and compared for supporting the decision making process.

6. Conclusion

The target-based approach for multi-hazard analysis presented in this paper is a tool to support decision makers for evaluating, in an integrated way, the output of multiple single-hazard assessments. The method is based on a probabilistic assessment of a FT, which can be directly implemented to analyze hazards related to different sources (e.g. volcanic, climate-related, tectonic, etc.). However, when considering different volcanic hazards related to activity of the same volcano, as in this work, a common cause effect may undermine the independence assumption for setting the BEs, requiring special attention to avoid potential biases due to possible correlations between hazard occurrences at a given location.

The example shown in the case study provides some clues about the added value of the information that can be available to a decision maker using the proposed approach: (i) adopting a target-based approach, the analyst first focuses on identifying, for each hazard, the critical threshold of the intensity measure that is relevant for the specific TO under study; this enormously simplifies the work of the analyst because it allows the decision maker to focus on the relevant data and related uncertainty and avoid them to deal with full hazard curves; (ii) as can be seen in Fig. 1, different hazards provide different information relevant for the TO under analysis; after evaluating the identified logical relationships (using the fault tree), an integrated probabilistic assessment is produced, which provides an objective and transparent assessment of the probability associated with the TO, as well as the related uncertainties derived (and propagated) from the uncertainties of the single hazard assessments (Fig. 4). Comparing Figs. 1 and 4, it is possible to figure out how the landscape of the results changes when comparing each single hazard with the final multi-hazard analysis; in our example, the probabilities of the TO under study have values that are about one order of magnitude greater than the higher single hazards (tephra and seismic), immediately highlighting the hotspots of the potentially critical areas (according to the situation set in the TO definition). Such results have the added value that, given the single hazards, the critical thresholds, and the logical fault tree adopted, the results are data driven and fully reproducible, avoiding subjective choices as the definition of weights or the creation of indexes (as often done in multi-hazard analyses, see e.g. Thierry et al., 2008, Totaro et al., 2020, Gjerløw et al., 2022).

We argue that the findings shown in this paper underscore the advantages of adopting the proposed approach for supporting decision makers to perform tasks of planning, mitigation, or emergency preparedness. The output relies on the quality of probabilistic single hazard assessments, and on the proper definition of the scenario for assessing the target objective of interest. The approach has been developed in the framework of a research project focusing on the volcano-induced multi-hazard and multi-risk assessment at Etna, which is particularly challenging because of possible correlations threatening the assumption of independence of BEs; however, the flexibility of the proposed approach allows it to be easily extended to any other natural hazards, such as tsunamis, landslides, floods, and extreme weather events, among others.

Data availability statement. Data of the single hazard assessments used in this work are available from the publications presented in this volume for the probabilistic single hazard assessment (Cappello et al., 2025, for the lava, Scollo et al., 2025, for the tephra, and D'Amico et al., 2025, for the seismic hazard).

Acknowledgements. This work was supported by the INGV project Pianeta Dinamico (CUP D53J19000170001) funded by MIUR ("Fondo finalizzato al rilancio degli investimenti delle amministrazioni centrali dello Stato e allo sviluppo del Paese", legge 145/2018), Tema 8 – PANACEA 2021-23. The quantitative evaluation of the Fault-trees for MH assessment has been performed adapting the tool developed by Garcia-Aristizabal et al. (2019), which is freely available in the EPOS (European Plate Observing System) infrastructure of the Thematic Cor Services "Anthropogenic Hazards" (available at the site: https://tcs.ah-epos.eu/episodes/). The maps presented in this paper were produced using QGIS Geographic Information System (Open Source Geospatial Foundation Project. http://qgis.org).

References

Alcozer-Vargas, N. M., P. Reyes-Hardy, A. Esquivel and F. Aguilera (2022). A GIS-based multi-hazard assessment at the San Pedro volcano, Central Andes, northern Chile, Front. Earth Sci., 10, doi:10.3389/feart.2022.897315.

Andronico, D., S. Scollo, S. Caruso and A. Cristaldi (2008). The 2002-03 etna explosive activity: Tephra dispersal and features of the deposits, J. Geophys. Res. Solid Earth, 113, B4, doi:10.1029/2007JB005126.

Azzaro, R. and S. D'Amico (2014). Catalogo Macrosismico dei Terremoti Etnei (CMTE), 1633-2023 [Data set], Istituto Nazionale di Geofisica e Vulcanologia (INGV), doi:10.13127/cmte.

Azzaro, R. and M. S. Barbano (1996). Relationship between Seismicity and Eruptive Activity at Mt. Etna volcano (Italy) as Inferred from Historical Record Analysis: The 1883 and 1971 Case Histories, Ann. Geophys., 39, 2, doi:10.4401/ag-3981.

Bedford, T. and R. Cooke (2001). Probabilistic risk analysis: foundations and methods, Cambridge University Press, Cambridge, doi:10.1017/CBO9780511813597.

Bevilacqua, A., R. Azzaro, S. Branca, S. D'Amico et al. (2022). Quantifying the statistical relationships between flank eruptions and major earthquakes at Mt. Etna volcano (Italy), J. Geophys. Res. Solid Earth, 127, e2022JB024145, doi:10.1029/2022JB024145.

Biass, S., C. Bonadonna, L. Connor and C. Connor (2016). Tephraprob: a matlab package for probabilistic hazard assessments of tephra fallout, J. Appl. Volcanol., 5, 10, doi:10.1186/s13617-016-0050-5.

Bilotta, G., A. Cappello and G. Ganci (2023). Formal matters on the topic of risk mitigation: A mathematical perspective, Appl. Sci., 13, 1, doi:10.3390/app13010265.

Branca, S. and T. Abate (2017). Current knowledge of Etna's flank eruptions (Italy) occurring over the past 2500 years. From the iconographies of the XVII century to modern geological cartography, J. Volcanol. Geotherm. Res., doi:10.1016/j.jvolgeores.2017.11.004.

Branca, S., E. De Beni, D. Chester, A. Duncanet et al. (2017). The 1928 eruption of mount Etna (Italy): Reconstructing lava flow evolution and the destruction and recovery of the town of Mascali, J. Volcanol. Geotherm. Res., 335, 54-70, doi:10.1016/j.jvolgeores.2017.02.002.

Cappello, A., G. Bilotta, F. Zuccarello, C. Proietti et al. (2025). An improved methodology for lava flow hazard mapping at Etna volcano, Ann. Geophys., 68, doi:10.4401/ag-9157.

Cappello, A., G. Bilotta and G. Ganci (2022). Modeling of geophysical flows through GPUFLOW, Appl. Sci., 12, 4395, doi:10.3390/app12094395.

Centorrino, V., G. Bilotta, A. Cappello, G. Ganci et al. (2021). A particle swarm optimization-based heuristic to optimize the configuration of artificial barriers for the mitigation of lava flow risk, Environ. Model. Softw., 139, 105023, doi:10.1016/j.envsoft.2021.105023.

Coltelli, M., M. Marsella, C. Proietti and S. Scifoni (2012). The case of the 1981 eruption of mount Etna: An example of very fast moving lava flows, Geochem. Geophys. Geosyst., 13, 1, doi:10.1029/2011GC003876.

Connor, C. B., B. E. Hill, B. Winfrey, M. N. Franklin et al. (2001). Estimation of volcanic hazards from tephra fallout, Nat. Hazard Rev., 33-42, doi:10.1061/(ASCE)1527-6988(2001)2:1(33).

D'Amico, V. and D. Albarello (2008). SASHA: a computer program to assess seismic hazard from intensity data, Seismol. Res. Lett., 79, 5, 663-671, doi:10.1785/gssrl.79.5.663.

D'Amico, S., R. Azzaro, G. Tusa, T. Tuvè et al. (2025). Volcano-tectonic seismicity and related hazard: a component of the multi-hazard assessment in the highly exposed region of Mt. Etna (Italy), Ann. Geophys., 68, doi:10.4401/ag-9152.

Ganci, G., A. Cappello and M. Neri (2023). Data Fusion for Satellite-Derived Earth Surface: The 2021 Topographic Map of Etna Volcano, Remote Sens., 15, 198, doi:10.3390/rs15010198.

Garcia-Aristizabal, A., J. Kocot, R. Russo and P. Gasparini (2019). A probabilistic tool for multi-hazard risk analysis using a bow-tie approach: application to environmental risk assessments for geo-resource development projects, Acta Geophys., 67, 1, 385-410, doi:10.1007/s11600-018-0201-7.

Grünthal, G. (1998). European macroseismic scale 1998 (EMS-98), in Cahiers du Centre Européen de Géodynamique et de Séismologie, 15, Luxembourg, Conseil de l'Europe.

Gasparini, P. and A. Garcia-Aristizabal (2014). Seismic Risk Assessment, Cascading Effects, in Encyclopedia of Earthquake Engineering M. Beer, I. A. Kougioumtzoglou, E. Patelli and I. S. K. Au (Editors), Springer, Berlin Heidelberg, 1-20, doi:10.1007/978-3-642-35344-4_260.

Gelman, A. J. Carlin, H. Stern and D. Rubin (1995). Bayesian data analysis, Chapman and Hall, 552, doi:10.1201/9780429258411.

Gjerløw, E., A. Hoskuldsson, S. Bartolini, S. Biass et al. (2022). The volcanic hazards of Jan Mayen Island (North-Atlantic), Front. Earth Sci., 10, doi:10.3389/feart.2022.730734.

Liu, Z., F. Nadim, A. Garcia-Aristizabal, A. Mignan et al. (2015). A three-level framework for multi-risk assessment, Georisk: Assessment and Management of Risk for Engineered Systems and Geohazards, 9, 2, 59-74, doi:10.1080/17499518.2015.1041989.

Martín-Raya, N., J. Díaz-Pacheco and A. López-Díez (2024). A. Multi-hazard risk assessment analysis in La Palma: an approach for risk mitigation, Geoenviron. Disasters, 11, 33, doi:10.1186/s40677-024-00296-3.

Martinez Montesinos, B., M. T. Luzon, L. Sandri, O. Rudyy et al. (2022). On the feasibility and usefulness of high-performance computing in probabilistic volcanic hazard assessment: An application to tephra hazard from Campi Flegrei, Front. Earth Sci., 10, doi:10.3389/feart.2022.941789.

Marzocchi, W., A. Garcia-Aristizabal, P. Gasparini, M. L. Mastellone et al. (2012). Basic principles of multi-risk assessment: a case study in Italy, Nat. Hazards, 62, 2, 551-573, doi:10.1007/s11069-012-0092-x.

Orlecka-Sikora, B., S. Lasocki, J. Kocot, T. Szepieniec et al. (2020). An open data infrastructure for the study of anthropogenic hazards linked to georesource exploitation, Sci. Data, 7, 1-16, doi:10.1038/s41597-020-0429-3.

Pessina, V., F. Meroni, E. Varini, M. Longoni et al. (2025). Probabilistic risk analysis due to volcanic-induced hazards at Mount Etna, Ann. Geophys., 68, 1, doi:10.4401/ag-9175.

Rausand, M. and A. Høyland (2004). System reliability theory: models, statistical methods and applications, Wiley-Interscience, Hoboken, 636, ISBN:047147133X.

Rotondi, R., E. Varini and C. Brambilla (2016). Probabilistic modelling of macroseismic attenuation and forecast of damage scenarios, Bull. Earthq. Eng., 14, 7, 1777-1796, doi:10.1007/s10518-015-9781-7.

Sandri, L., M. de' Michieli Vitturi, A. Costa, M. A. Di Vito et al. (2024). Lahar events in the last 2000 years from vesuvius eruptions – part 3: Hazard assessment over the campanian plain, Solid Earth, 15, 4, 459-476, doi:10.5194/se-15-459-2024.

Scollo, S., C. Bonadonna, A. Garcia, L. Mereu et al. (2025). New developments in the estimation of tephra fallout hazard at Mt. Etna, in Italy, during the PANACEA project, Ann. Geophys., 68, 1, doi:10.4401/ag-9174.

Selva, J., A. Costa, G. De Natale, M. Di Vito et al. (2018). Sensitivity test and ensemble hazard assessment for tephra fallout at Campi Flegrei, Italy, J. Volcanol. Geotherm. Res., 351, 1-28, doi:10.1016/j.jvolgeores.2017.11.024.

Selva, J. (2013). Long-term multi-risk assessment: statistical treatment of interaction among risks, Nat. Hazards 67, 701-722, doi:10.1007/s11069-013-0599-9.

Siu, N. O. and D. L. Kelly (1998). Bayesian parameter estimation in probabilistic risk assessment, Reliab. Eng. Syst. Saf., 62, 1, 89-116, doi:10.1016/S0951-8320(97)00159-2.

Thierry, P., L. Stieltjes, E. Kouokam, P. Ngueya et al. (2008). Multi-hazard risk mapping and assessment on an active volcano: the GRINP project at Mount Cameroon, Nat. Hazards, 45, 3, 429-456, doi:10.1007/s11069-007-9177-3.

Tonini, R., L. Sandri and M. A. Thompson (2015). Pybetvh: a python tool for probabilistic volcanic hazard assessment and for generation of bayesian hazard curves and maps, Comput. Geosci., 79, 38-46, doi:10.1016/j.cageo.2015.02.017.

Totaro, F., I. Alberico, D. Di Martire, C. Nunziata et al. (2020). The key role of hazard indices and hotspot in disaster risk management: the case study of Napoli and Pozzuoli municipalities (southern Italy), J. Maps, 16, 2, 68-78, doi:10.1080/17445647.2019.1698472.

Weir, A. M., S. Mead, M. S. Bebbington, T. M. Wilson et al. (2022). A modular framework for the development of multi-hazard, multi-phase volcanic eruption scenario suites, J. Volcanol. Geotherm. Res., 427, 107557, doi:10.1016/j.jvolgeores.2022.107557.

Zuccarello, F., G. Bilotta, G. Ganci, C. Proietti et al. (2023). Assessing impending hazards from summit eruptions: the new probabilistic map for lava flow inundation at Mt. Etna, Sci. Rep., 13, 19543, doi:10.1038/s41598-023-46495-0.

***CORRESPONDING AUTHOR: Alexander GARCIA**,
Istituto Nazionale di Geofisica e Vulcanologia, Sezione di Bologna, Bologna, Italy
e-mail: alexander.garcia@ingv.it